Excitatory synaptic activity is associated with a rapid structural plasticity of inhibitory synapses on hippocampal CA1 pyramidal cells

---

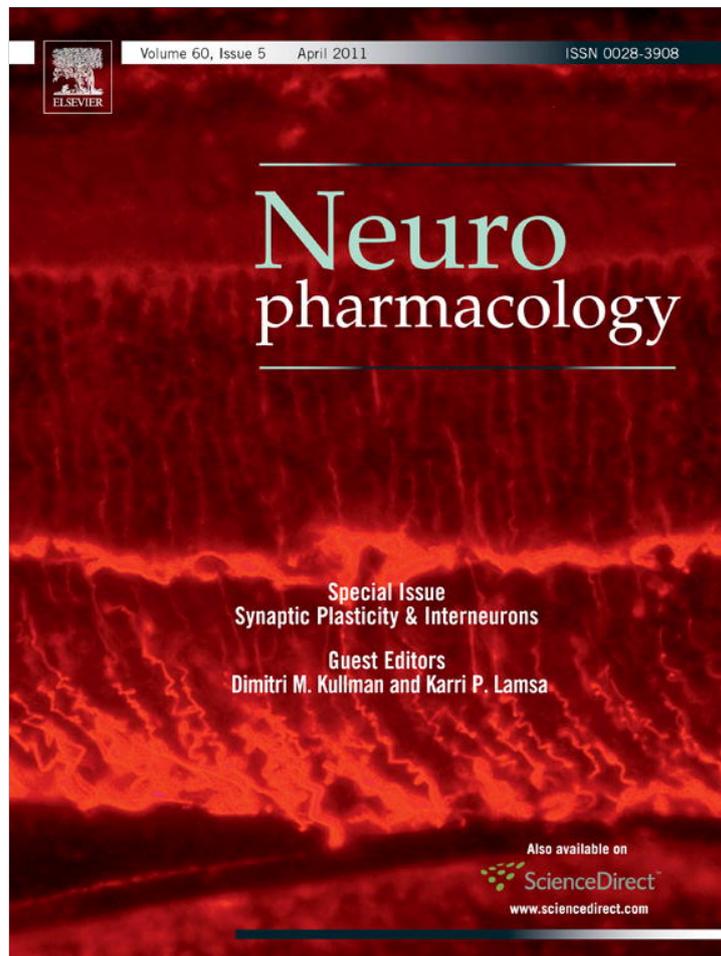Lushnikova, Irina; Skibo, Galina; Muller, Dominique; Nikonenko, Iryna

Excitatory synaptic activity is associated with a rapid structural plasticity of inhibitory synapses on hippocampal CA1 pyramidal cells

Irina Lushnikova [a], Galina Skibo [a], Dominique Muller [b], Irina Nikonenko [b,*]

[a] Department of Cytology, Bogomoletz Institute of Physiology, Bogomoletz street 4, 01024 Kiev, Ukraine
[b] Department and Center of Neuroscience, Geneva University Medical Center, 1 rue Michel Servet, 1211 Geneva 4, Switzerland

A R T I C L E   I N F O

A B S T R A C T

Synaptic activity, such as long-term potentiation (LTP), has been shown to induce morphological plasticity of excitatory synapses on dendritic spines through the spine head and postsynaptic density (PSD) enlargement and reorganization. Much less, however, is known about activity-induced morphological modifications of inhibitory synapses. Using an *in vitro* model of rat organotypic hippocampal slice cultures and electron microscopy, we studied activity-related morphological changes of somatic inhibitory inputs triggered by a brief oxygen–glucose deprivation (OGD) episode, a condition associated with a synaptic enhancement referred to as anoxic LTP and a structural remodeling of excitatory synapses. Three-dimensional reconstruction of inhibitory axo-somatic synapses at different times before and after brief OGD revealed important morphological changes. The PSD area significantly and markedly increased at synapses with large and complex PSDs, but not at synapses with simple, macular PSDs. Activity-related changes of PSD size and presynaptic bouton volume developed in a strongly correlated manner. Analyses of single and serial sections further showed that the density of inhibitory synaptic contacts on the cell soma did not change within 1 h after OGD. In contrast, the proportion of the cell surface covered with inhibitory PSDs, as well as the complexity of these PSDs significantly increased, with less macular PSDs and more complex, segmented shapes. Together, these data reveal a rapid activity-related restructuring of somatic inhibitory synapses characterized by an enlargement and increased complexity of inhibitory PSDs, providing a new mechanism for a quick adjustment of the excitatory–inhibitory balance.

This article is part of a Special Issue entitled 'Synaptic Plasticity & Interneurons'.

1. Introduction

Structural and functional plasticity of excitatory synapses is assumed to play a major role as a physiological mechanism underlying learning and memory (reviewed in Alvarez and Sabatini, 2007). Changes in synaptic strength, but also remodeling of excitatory synapses, including enlargement of dendritic spine heads, modifications of the postsynaptic density or growth of new protrusions, have been largely described as a result of application of high frequency stimulation patterns or other activity paradigms such as short anoxic/hypoglycemic episodes or seizure induction (Buchs and Muller, 1996; Jourdain et al., 2002; Bourne and Harris, 2008). Far less is known about modifications of inhibitory synapses under similar conditions of activity, although inhibitory inputs play a crucial role in shaping the activity of neuronal networks (Cobb et al., 1995; Freund and Buzsaki, 1996; reviewed in

Freund, 2003; Klausberger and Somogyi, 2008). Long-term changes of interneuron discharge and of inhibitory transmission associated with increased synaptic activity have been reported at various inhibitory synapses (Buzsaki and Eidelberg, 1982; Gaiarsa et al., 2002; Kullmann and Lamsa, 2007; Klausberger and Somogyi, 2008; Pelletier and Lacaille, 2008; McBain and Kauer, 2009; Nissen et al., 2010). The cellular and molecular mechanisms underlying these phenomena are however still poorly understood and rely on both pre- and postsynaptic modifications depending on the synapses under study. Similarly, the issue of whether structural remodeling of inhibitory synapses also occurs under conditions that induce structural plasticity of excitatory synapses is yet unclear. A recent study indicates that an LTP-inducing theta-burst stimulation protocol results in parallel changes in excitatory and inhibitory synapse morphology and in particular in a reduction in number but increase in size of inhibitory synapses on distal dendrites of CA1 pyramidal neurons (Bourne and Harris, 2010). Here we used a brief oxygen–glucose deprivation (OGD) paradigm that promotes a very large scale strengthening and remodeling of excitatory synapses

and electron microscopy (EM) to examine whether morphological modifications of axo-somatic inhibitory synapses take place at the level of hippocampal CA1 pyramidal neuron somata, where inhibitory contacts are concentrated. Our data demonstrate a rapid activity-related structural plasticity of inhibitory synapses that may contribute to the maintenance of the balance between excitation and inhibition.

2. Methods

2.1. Organotypic hippocampal slice cultures

Hippocampal organotypic slice cultures were prepared from 7 days old rat pups as described (Stoppini et al., 1991), according to a protocol approved by the Geneva Veterinarian Office (authorization 31.1.1007/3520/0), and maintained in culture for 10–13 days before experiments. The use of organotypic cultures as a model system facilitated experimental manipulations and allowed us to limit the number of animals used for the study.

2.2. Induction of anoxic LTP by brief oxygen–glucose deprivation

Brief oxygen–glucose deprivation episode was applied to induce the anoxic LTP (Hammond et al., 1994; Hsu and Huang, 1997; Jourdain et al., 2002). The organotypic cultures grown on confetti cut from porous Millipore membranes (Millipore) were placed in an interface chamber perfused with an artificial cerebro-spinal medium containing (in mM): 124 NaCl, 1.6 KCl, 2.5 CaCl$_2$, 1.5 MgCl$_2$, 24 NaHCO$_3$, 1.2 KH$_2$PO$_4$, 2 ascorbic acid, and 10 glucose (pH 7.4; 32 °C), bubbled with a gas mixture containing 95% O$_2$ and 5% CO$_2$ (Jourdain et al., 2002). Short episodes of oxygen–glucose deprivation were produced by switching to a medium containing 10 mM sucrose instead of glucose and exposing the slice cultures to an atmosphere composed of 95% N$_2$, 5% CO$_2$ for 10 min, followed by recovery under the standard conditions in the incubator for 30 or 60 min before fixation for EM. Ten minutes exposure to OGD in the interface configuration induces robust and long-lasting LTP (Jourdain et al., 2002), while shorter OGD episodes in this configuration were unable to induce sufficient potentiation (unpublished observations).

2.3. Electron microscopy processing

The cultures were fixed and processed for EM using a classic EPON embedding protocol. Before ultra-thin cutting, the semi-thin sections (2 μm) were cut from all cultures, stained with methylene blue and examined with light microscopy. For 3D reconstructions, ribbons of ultra-thin sections (60 nm; ultratome Ultracut-E; Reichert-Jung) were cut at the depth of 40–60 μm from the membrane side of the culture, in the CA1 stratum pyramidale, collected on single-slot Formvar-coated copper grids and stained for 20 min in 5% uranyl acetate and 30 s in lead citrate. From each slice culture, 40–50 ultra-thin sections were cut. The preparations were examined using Tecnai G^{2}12 transmission electron microscope (FEI Company; Eindhoven, Netherlands) equipped with a digital camera Mega View III (Soft Imaging Systems, Munster, Germany), and the serial images were taken at magnification of ×23,000. For the synapse density and PSD fraction estimations on the single sections, the thin and ultra-thin sections from pyramidal CA1 layer were cut from the same culture at different angles, to avoid possible orientation bias. For each experimental group, 3 slice cultures from different experiments were cut and analyzed. The single images were taken from randomly spotted pyramidal cell bodies at magnification of ×9700. The data were expressed as the number of synapses (presynaptic terminals facing a postsynaptic density) or fraction of PSD per micrometer of a cell body membrane profile.

2.4. Immunogold staining for γ-aminobutyric acid (GABA)

Identification of inhibitory GABAergic synapses was carried out with post-embedding immunogold staining as described (Buckmaster et al., 2002). Briefly, grids with ultra-thin sections were washed in saline containing 0.05 M Tris and 0.1% Triton X-100 (TBST, pH = 7.6), incubated in blocking solution (10% normal goat serum (NGS) in TBST) for 1 h, and in primary antibodies (mouse monoclonal anti-GABA, Sigma; 1:200 in TBST containing 2% NGS) overnight, at 4 °C. After a thorough wash, the grids were incubated during 1 h with anti-mouse IgG conjugated to 15 nm gold particles (BBInternational; 1:40 in TBST containing 1% BSA, pH = 8.2), and thoroughly washed. The images of the labeled synapses were taken at magnification of ×23,000.

2.5. Morphological analysis and three-dimensional reconstructions

Inhibitory (symmetric) synapses were defined by the presence of a thin PSD facing an active zone of the similar thickness, with at least three presynaptic vesicles. Complex PSDs were defined by the presence of a discontinuity on a single section. Inhibitory presynaptic terminals were identified by the presence of an enlargement of the axonal shaft containing pleomorphic synaptic vesicles and facing at least one symmetric PSD. The apposition zone of the presynaptic terminal to the cell body was estimated as a total area of contact between the membranes of these two structures. The synapse profiles were photographed serially, aligned, reconstructed and analyzed using software Reconstruct developed by J.C. Fiala and K.M. Harris (RECONSTRUCTTM available for download at http://synapses.clm.utexas.edu/tools/reconstruct/reconstruct.stm; Fiala and Harris, 2001; Fiala, 2005).

For each condition, 30 synapses with a simple PSD and 20 synapses with a complex PSD, selected randomly, were 3D reconstructed and analyzed.

2.6. Statistical analysis

Data are shown as mean ± SEM. Statistical analyses were performed using the Kolmogorov–Smirnov non-parametric two-sample test.

3. Results

3.1. Axo-somatic inhibitory synapses

Previous work has shown that application of a brief OGD to hippocampal slices results in a lasting increase of excitatory synaptic strength, mimicking theta burst-induced LTP and without effects on immediate cell survival (Crepel et al., 1993; Hammond et al., 1994; Hsu and Huang, 1997; Jourdain et al., 2002). This lasting synaptic potentiation was therefore called anoxic LTP. Like theta burst-induced LTP, brief OGD-mediated potentiation is NMDA and calcium dependent and accompanied by excitatory synapse remodeling and spine growth (Jourdain et al., 2002). Additionally, an important advantage of this protocol is that the changes in synaptic strength and ultrastructure are produced at a very large scale (Jourdain et al., 2002) thus making possible morphological analyses by random sampling of synaptic contacts.

Previous work reported that examination of slice cultures on semi-thin sections revealed no signs of acute cell damage or death of neurons within 1 h after the brief OGD episode (Jourdain et al., 2002). Consistent with this finding, we did not detect signs of cell damage by electron microscopic analysis of CA1 pyramidal cell bodies and interneurones in this study. In order to verify this further, we measured the diameter of CA1 pyramidal cell bodies on the semi-thin (2 μm) sections from EPON-embedded slices (3 slices per condition, 50 neurons per slice; in total, 150 pyramidal cell bodies per condition). This analysis confirmed that brief OGD episode did not induce detectable changes in cell body dimensions (minimum and maximum diameters measured for each cell were: 13.2 ± 0.2 and 21.5 ± 0.3 μm, under control conditions; 13.1 ± 0.2 and 21.4 ± 0.3 μm, 30 min after OGD; and 12.9 ± 0.2 and 21.0 ± 0.3 μm, 60 min after OGD).

Using this brief OGD stimulation paradigm, we examined how activity affected the morphological characteristics of inhibitory synapses present on the soma of CA1 pyramidal cells, comparing PSD size and shape, apposition zone and presynaptic terminal volume 30 and 60 min after OGD to non-stimulated controls. These time points were chosen based on our previous observations indicating a marked remodeling of excitatory CA1 synapses and the formation of new spines during the first hour following theta-burst stimulation (Toni et al., 1999, 2001) or brief OGD episode (Jourdain et al., 2002). We took special care to correctly identify pyramidal cells in the CA1 region of organotypic hippocampal slice cultures. At the EM level, pyramidal cell bodies were defined by a typical pyramidal shape and by the presence of a large round nucleus, with homogeneously dispersed karyoplasm, that occupied much of the perikaryon. Inhibitory somatic synapses were identified by their morphology (Peters et al., 1991): symmetric synaptic contacts, with a narrow synaptic cleft and a postsynaptic density significantly less pronounced than in excitatory synapses, facing axonal terminals filled with pleomorphic synaptic vesicles (Fig. 1A). In order to validate these morphological criteria, a series of experiments was carried out with immunogold staining for GABA. As shown in Fig. 1,
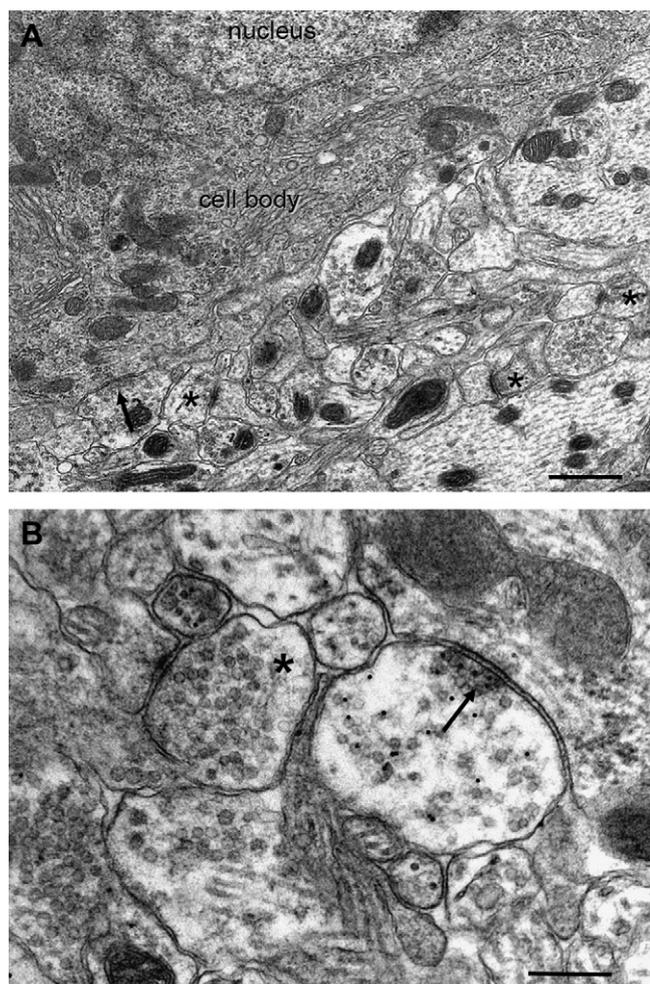
Fig. 1. Electron microscopy illustrations of the axo-somatic inhibitory synapses. Arrow points at the symmetric inhibitory synapse on pyramidal cell body in the CA1 hippocampal area. Compare with asymmetric excitatory synapses in the neuropil (A, asterisks). Post-embedding immunogold staining for GABA is present in the symmetric inhibitory synapse on the soma (arrow) but absent in the excitatory presynaptic terminal facing a thick PSD (asymmetric excitatory synapse, asterisk) in a dendritic spine (B). Scale bars: A - 1 μm; B - 0.25 μm.

gold particles were indeed observed in synapses identified using the above criteria as symmetrical or inhibitory, but absent in asymmetrical excitatory contacts (Fig. 1B).

3.2. Three-dimensional analysis of axo-somatic inhibitory synapses

Serial images were taken from randomly spotted inhibitory synaptic contacts on CA1 pyramidal cell bodies. Three-dimensional reconstructions of the apposition zone of the presynaptic terminal to the cell body, of the PSD and of the presynaptic bouton (Fig. 2A) revealed that transient OGD resulted in a progressive and significant increase of the PSD size of inhibitory synapses. The increase was detectable already at 30 min and became significant 1 h after treatment, averaging 58% when compared to non-stimulated controls (0.098 ± 0.008 μm^2, 0.119 ± 0.009 μm^2 and 0.155 ± 0.011 μm^2 in controls, 30 min and 60 min after OGD respectively; Fig. 2B). The general size of the inhibitory synaptic complexes also showed a tendency to enlargement at this time-point, with an increase of the apposition zone by around 23% and of the presynaptic terminal volume by 20.6%, although these changes were not statistically significant (apposition zone: 0.356 ± 0.029 μm^2

and 0.438 ± 0.028 μm^2; presynaptic terminal volume: 0.161 ± 0.012 μm^3 and 0.194 ± 0.015 μm^3, in controls and 60 min after stimulation, respectively; Fig. 2B and C). Three-dimensional analysis of somatic inhibitory PSDs showed a high diversity of shapes, including simple, macular (Fig. 1), but also complex shapes, with discontinuities of the PSD on single sections. 3D reconstruction of these PSDs revealed complex, non-macular shapes, referred to as perforated PSDs (Fig. 3A), or PSDs with a complete fragmentation of the synaptic contact and separate pools of synaptic vesicles facing each part of the PSD (segmented PSDs; Fig. 2A; Fig. 3A). Under control conditions, PSDs with complex shapes revealed by 3D reconstruction were on average almost two times larger than macular ones (0.075 ± 0.007 μm^2 and 0.133 ± 0.012 μm^2, respectively; $p < 0.05$; Fig. 3B). Synapses with simple PSDs were also associated with significantly smaller presynaptic terminals (0.129 ± 0.013 μm^3 and 0.209 ± 0.019 μm^3 in simple and complex synapses, Fig. 3D) and with smaller apposition zones (0.269 ± 0.025 μm^2 and 0.488 ± 0.046 μm^2; Fig. 3C). In general, there was a positive correlation between the size of the inhibitory PSD and the volume of the presynaptic terminal contacting it ($r = 0.66$).

### 3.3. Activity-dependent remodeling of inhibitory synapses

We then analyzed separately the parameters of simple and complex synapses, under conditions of brief OGD. These experiments revealed a marked enlargement of the PSDs for the synapses with complex PSDs (71.5% increase 1 h after stimulation when compared to the values obtained in non-stimulated controls: 0.228 ± 0.016 μm^2 and 0.133 ± 0.012 μm^2 respectively; $p < 0.05$), while in the synapses with simple PSDs the changes were not significant (Fig. 3B). The apposition zone and presynaptic terminal volume in the synapses with complex PSDs also significantly increased at 1 h (from 0.488 ± 0.046 μm^2 to 0.628 ± 0.028 μm^2 and from 0.209 ± 0.019 μm^3 to 0.275 ± 0.021 μm^3; Fig. 3C and D), the changes averaging 28.8% and 31.3%, respectively. The differences in apposition zone or terminal volume for synapses with simple PSDs were not significant. These activity-dependent modifications of the sizes of inhibitory PSDs and of related presynaptic terminals showed a strong correlation at both times analyzed after stimulation ($r = 0.89$, 30 min after brief OGD, and $r = 0.84$, 60 min after stimulation). Together, these experiments show that brief OGD is associated with marked enlargement of inhibitory contacts affecting primarily synapses with complex PSDs.

3.4. Synapse density, PSD coverage and type

Next, we investigated whether synaptic activity could induce formation of new inhibitory synaptic contacts on CA1 pyramidal cells within our experimental time frame. The number and size of inhibitory synapses per micrometer of cell body length was estimated on random single sections of the CA1 pyramidal cells (Fig. 1A) by measuring the number of presynaptic terminals facing inhibitory PSDs and fraction length of somatic membrane covered by inhibitory PSDs. We analyzed 100 images per condition representing a total length of the soma contour of 1450 μm for controls, 1489 μm 30 min after and 1480 μm 1 h after a brief OGD. These measurements showed that the number of inhibitory terminals per 100 μm of somatic membrane did not change after stimulation with respect to non-stimulated controls (Fig. 4A). However, the total coverage of somatic membrane by inhibitory PSDs (measured as PSD length per μm of cell body profile length) increased, consistent with the enlargement of synapses reported above (from 0.030 ± 0.002 μm in controls to 0.041 ± 0.002 μm 1 h after stimulation; Fig. 4B). Additionally, an important change concerned the type of inhibitory synapses as determined by the presence of
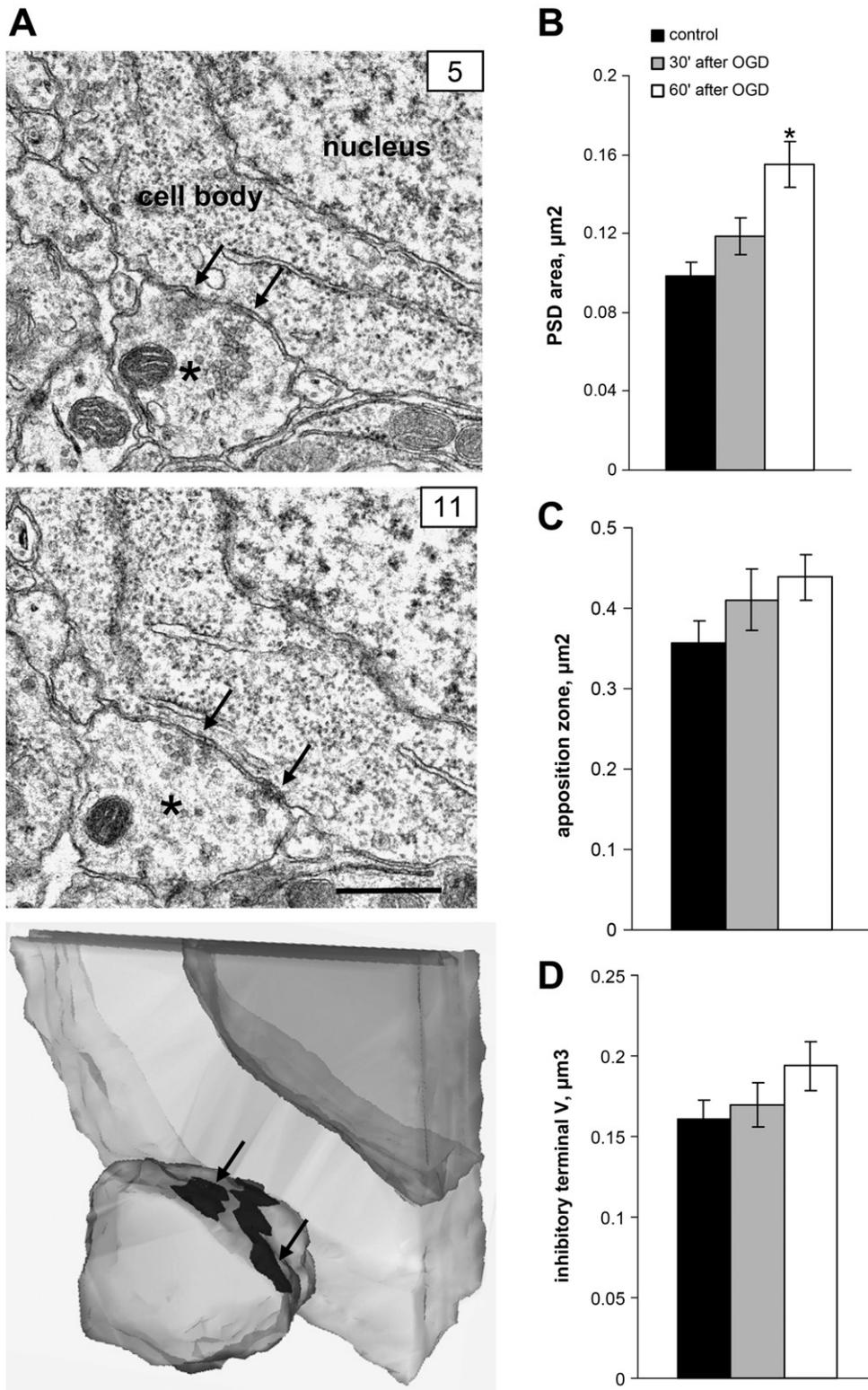
Fig. 2. Three-dimensional reconstructions reveal structural modifications of the inhibitory synapses induced by the brief OGD episode. Serial EM images of the axo-somatic symmetric synapse (asterisks) and 3D reconstruction of this synapse are illustrated in A. The number of the image in the series is shown in the insets. Note a discontinuity (segmentation) of the PSD visible on the EM images and on the 3D reconstruction and clear separation of synaptic vesicle pools between two parts (arrows) of this complex segmented PSD. PSD area (in μm^2, B), the area of the apposition zone of the presynaptic terminal to the soma (in μm^2, C) and the presynaptic terminal volume (in μm^3, D) under control conditions (black bars), 30 min (gray bars) and 60 min (white bars) after brief OGD. Data represent the mean ± SEM, measured in 50 synapses for each condition; *indicates statistical significance ($p < 0.05$) comparing to controls, by Kolmogorov–Smirnov two-sample test. Scale bar in A - 0.5 μm.
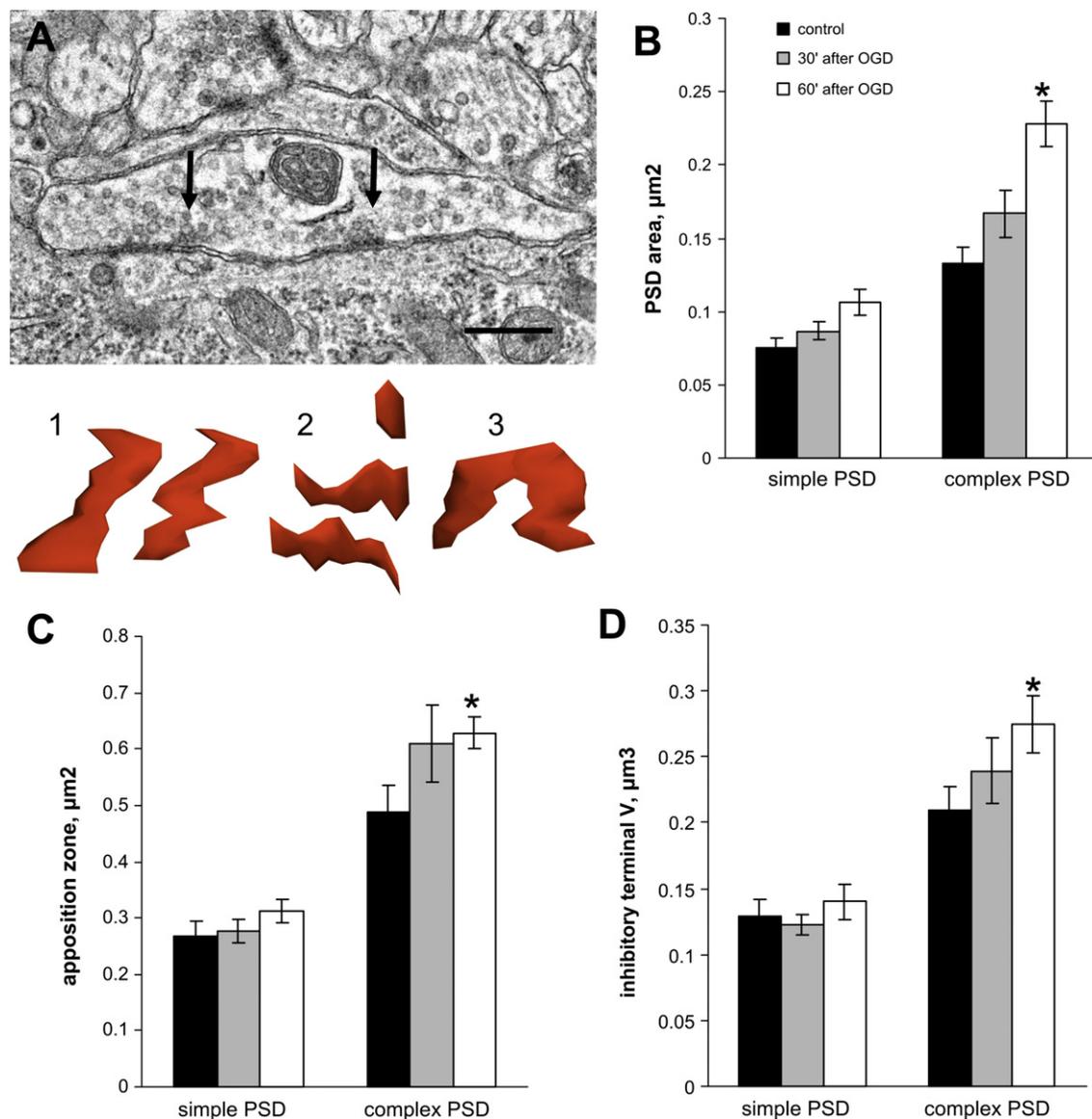
Fig. 3. Activity induces more pronounced restructuring of the inhibitory synapses with complex PSDs. EM illustration of a symmetric synapse with a complex PSD and separate synaptic vesicle pools (arrows) is shown on the top and examples of the 3D reconstructions of the complex segmented (1–2) and perforated (3) inhibitory PSDs on the cell bodies are presented underneath (A). Example 1 corresponds to the synapse illustrated on EM. Activity induces preferential enlargement of the PSD area of the complex synapses (B), as well as their apposition zone between a presynaptic terminal and a pyramidal cell soma (C) and the volume of the corresponding presynaptic inhibitory terminal (D). Data represent the mean ± SEM; *indicates statistical significance ($p < 0.05$) comparing to controls, by Kolmogorov–Smirnov two-sample test. Scale bar in A - 0.25 μm.

complex PSDs. Under control conditions, complex (discontinuous on a single section) PSD profiles represented 17.2% of all synapses. Following a brief OGD, this proportion significantly increased, by 66.5% at 30 min and by 142% at 1 h, representing respectively 28.3% and 38.2% of total inhibitory synapses (Fig. 4C and D). Conversely, macular PSD profiles were less numerous and decreased by 18.3% 1 h after stimulation. We further verified these measurements on serial sections, by tracing 30 randomly selected inhibitory contacts for each experimental condition through adjacent consecutive sections in order to determine the types of the PSDs (simple or complex) and their proportion within this random sample. This analysis provided ratios of simple and complex PSDs very similar to those obtained by single section assessment (compare Fig. 4D and E). Three-dimensional analysis of the complex synapses observed after stimulation showed a significant trend to formation of segmented PSDs, since their proportion increased from 25% under

control conditions to 45% at 1 h (Fig. 4F). Together, these data indicate that synaptic activity was not associated with an increase in inhibitory synapse number on CA1 pyramidal cell soma, but promoted their enlargement and transformation into complex, often segmented synapses.

4. Discussion

Hippocampal interneurons have extensive axonal arbors and innervate multiple pyramidal cells providing regulation of the overall level of excitability and synchronization in the network. The inhibitory input on the perisomatic region of a hippocampal CA1 pyramidal neuron originates primarily from basket cells (Freund and Buzsaki, 1996; Somogyi and Klausberger, 2005; Klausberger and Somogyi, 2008) and constitutes around 40% of all inhibitory synapses on a pyramidal cell (Megias et al., 2001). Because of the
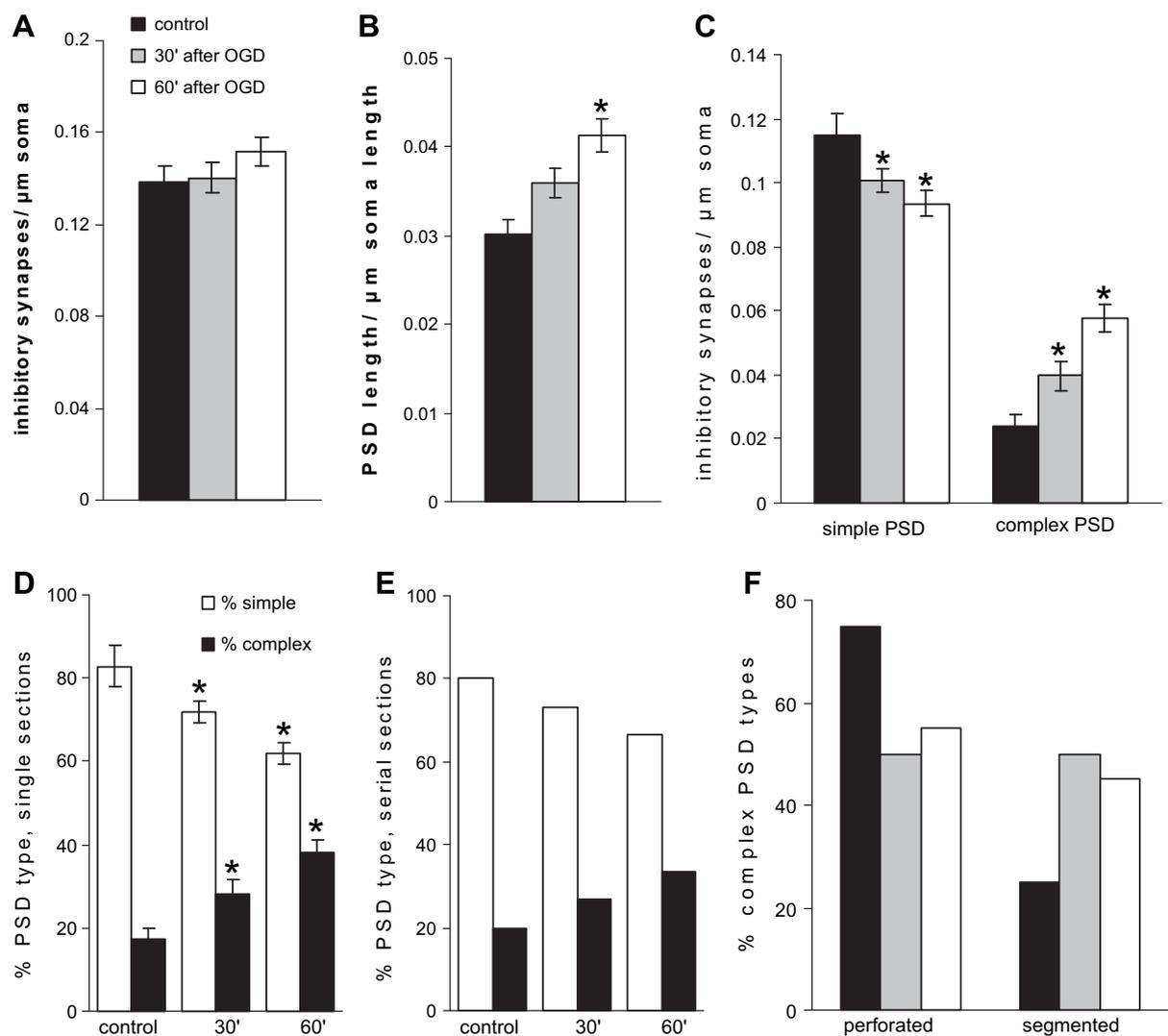
Fig. 4. Synaptic activity increases the complexity of the inhibitory PSDs. The total linear density of axo-somatic inhibitory terminals per μm of the soma profile remains stable (A), but synaptic coverage of the soma, measured as the length of PSD per μm of the soma profile, increased after brief OGD episode (B). The density of the simple synapses per μm of the soma profile decreases, while the density of the complex synapses increases after stimulation (C). Proportion of complex PSDs increases, as measured on single (D) and serial sections (E). Synaptic activity also induces segmentation of the complex PSDs (F). Data represent the mean ± SEM; *indicates statistical significance ($p < 0.05$) comparing to controls, by Kolmogorov–Smirnov two-sample test.

importance of this perisomatically clustered inhibition for the control of individual neurons output and of network activity (Cobb et al., 1995; Miles et al., 1996; reviewed in Bartos et al., 2007), we have chosen to analyze structural modifications of inhibitory synapses on the pyramidal cell soma under exposure to a brief OGD, a condition that has previously been shown to affect a large fraction of excitatory synapses, modifying both their strength and morphology.

Three-dimensional reconstructions of inhibitory synapses on CA1 pyramidal cell bodies revealed a high variability of inhibitory PSD shapes and sizes under control conditions. Along with simple (macular) PSDs, we also detected a significant fraction of synapses with complex (perforated or segmented) shapes, which were, on average, 1.8 times larger than simple ones. Complex PSDs were initially described at excitatory synapses on dendritic spines, where they are present under control conditions (Harris et al., 1992), but increase in number following induction of plasticity (Geinisman, 1993; Toni et al., 1999, 2001; Ganeshina et al., 2004; Stewart et al., 2005). They have been therefore considered as a plausible

morphological correlate of synapse strengthening, possibly reflecting the increased number of AMPA receptors expressed at potentiated synapses (Bourne and Harris, 2008). Our experiments reveal that at symmetric, inhibitory synapses, the postsynaptic densities are also sometimes disposed as discrete patches facing the same terminal, consistent with the observation of interruptions of the PSD on random single sections (Peters et al., 1991). Three-dimensional reconstructions illustrate the complexity of some inhibitory somatic PSDs, demonstrating the existence of separate release pools of synaptic vesicles attached to each part of a segmented inhibitory PSD. These experiments also reveal the correlation existing between PSD size and complexity and the volume of the presynaptic terminals facing these synapses.

The information regarding the effect of activity on the structural plasticity of inhibitory synapses is rather scarce, and mostly comes from light microscopy studies. Under conditions of chronic activity blockade in neuronal and organotypic cultures from hippocampus, the amount of inhibition and density of GABAergic terminals were reported to decrease (Marty et al., 2000; Hartman et al., 2006).

In contrast, chronic activity or repetitive activation such as occurs with kindling has been shown to lead to a strengthening of inhibitory synaptic inputs, an enlargement of apposition zones and an increase in the number of $GABA_A$ receptors at inhibitory synapses, detected both with light microscopy and EM (Nusser et al., 1998; Marty et al., 2004). These results thus point to the existence of mechanisms regulating the number of receptors expressed at inhibitory synapses and possibly controlled by ubiquitination processes (Saliba et al., 2007). Additionally, there is also evidence that continuous whisker stimulation during 24 h increases inhibitory synapse number and density and the ratio of inhibitory to excitatory synapses on spines in stimulated barrels (Knott et al., 2002). In a recent EM study LTP induction by theta-burst stimulation was reported to result in a correlated structural plasticity of excitatory and inhibitory synapses on distal apical dendritic segments of the CA1 pyramidal cells (Bourne and Harris, 2010). The number of inhibitory synapses decreased and was counterbalanced by an increase in their PSD surface area. These new data suggest that excitatory activity can be associated in dendritic areas to correlative changes in inhibitory synapse number or morphology.

As neuronal firing is mainly controlled by somatic inhibition, an important question was therefore to understand whether such structural remodeling could also affect somatic inhibitory synapses. Our experiments provide the first direct evidence that this is indeed the case. We used an activation protocol that was previously shown to trigger a potentiation of excitatory synapses comparable to LTP and to also affect their morphology in a similar way (Jourdain et al., 2002). It seems likely that these brief OGD episodes promote an LTP-like phenomenon at a large number of excitatory synapses, increasing thereby excitability. As shown by our 3D-EM reconstruction experiments, this protocol resulted in a marked structural reorganization of somatic inhibitory synapses. The size of synapses with complex PSDs markedly increased, the total PSD area on somatic pyramidal membranes also enlarged and this was associated with a shift from simple synapses with macular PSDs to complex synapses with segmented PSDs. The overall number of inhibitory contacts was however not found to be modified. These results suggest that this activity protocol promoted a global enlargement and restructuring of a large fraction of existing inhibitory synapses. This conclusion is consistent with the notion that kindling and strong stimulation protocols can be associated with an increased expression of $GABA_A$ receptors and that inhibitory synapses can also undergo a lasting potentiation. The additional interesting information provided here is that the structural changes are quite rapid and share similarities with what has been reported at excitatory synapses under similar conditions. Namely, the increased number of synapses with complex and particularly segmented PSDs, also reported in many studies at excitatory synapses, could similarly reflect processes regulating the expression of receptors and specifically their enhanced trafficking. One possible interpretation of these results could therefore be that the structural rearrangements described here represent the morphological correlate of an enhanced $GABA_A$ receptor trafficking and inhibitory potentiation triggered by increased excitatory activity. Although we did not assess inhibitory activity in these experiments, these results suggest that this inhibitory structural plasticity could represent a compensatory mechanism to maintain and adapt the excitatory/inhibitory balance in the tissue. This also opens new interesting questions with regard to the mechanisms responsible for these changes.

Together, this study provides strong evidence that enhanced activity can be rapidly associated with an important structural remodeling of inhibitory synapses consistent with a synapse enlargement and increased efficacy of somatic inhibition. These results thus confirm the existence of correlative excitatory/ inhibitory structural adaptations that could play a central role in the maintenance of the excitatory/inhibitory balance.

References

Alvarez, V.A., Sabatini, B.L., 2007. Anatomical and physiological plasticity of dendritic spines. Annu. Rev. Neurosci. 30, 79–97.

Bartos, M., Vida, I., Jonas, P., 2007. Synaptic mechanisms of synchronized gamma oscillations in inhibitory interneuron networks. Nat. Rev. Neurosci. 8, 45–56.

Bourne, J.N., Harris, K.M., 2008. Balancing structure and function at hippocampal dendritic spines. Annu. Rev. Neurosci. 31, 47–67.

Bourne, J.N., Harris, K.M., 2010. Coordination of size and number of excitatory and inhibitory synapses results in a balanced structural plasticity along mature hippocampal CA1 dendrites during LTP. Hippocampus Jan 25. [Epub ahead of print].

Buchs, P.A., Muller, D., 1996. Induction of long-term potentiation is associated with major ultrastructural changes of activated synapses. Proc. Natl. Acad. Sci. U.S.A. 93, 8040–8045.

Buckmaster, P.S., Yamawaki, R., Zhang, G.F., 2002. Axon arbors and synaptic connections of a vulnerable population of interneurons in the dentate gyrus in vivo. J. Comp. Neurol. 445, 360–373.

Buzsaki, G., Eidelberg, E., 1982. Direct afferent excitation and long-term potentiation of hippocampal interneurons. J. Neurophysiol. 48, 597–607.

Cobb, S.R., Buhl, E.H., Halasy, K., Paulsen, O., Somogyi, P., 1995. Synchronization of neuronal activity in hippocampus by individual GABAergic interneurons. Nature 378, 75–78.

Crepel, V., Hammond, C., Krnjevic, K., Chinestra, P., Ben-Ari, Y., 1993. Anoxia-induced LTP of isolated NMDA receptor-mediated synaptic responses. J. Neurophysiol. 69, 1774–1778.

Fiala, J.C., 2005. Reconstruct: a free editor for serial section microscopy. J. Microsc. 218, 52–61.

Fiala, J.C., Harris, K.M., 2001. Extending unbiased stereology of brain ultrastructure to three-dimensional volumes. J. Am. Med. Inform. Assoc. 8, 1–16.

Freund, T., Buzsaki, G., 1996. Interneurons of the hippocampus. Hippocampus 6, 345–470.

Freund, T.F., 2003. Interneurons diversity series: Rhythm and mood in perisomatic inhibition. Trends Neurosci. 26, 489–495.

Gaiarsa, J.L., Caillard, O., Ben-Ari, Y., 2002. Long-term plasticity at GABAergic and glycinergic synapses: mechanisms and functional significance. Trends Neurosci. 25, 564–570.

Ganeshina, O., Berry, R.W., Petralia, R.S., Nicholson, D.A., Geinisman, Y., 2004. Synapses with a segmented, completely partitioned postsynaptic density express more AMPA receptors than other axospinous synaptic junctions. Neuroscience 125, 615–623.

Geinisman, Y., 1993. Perforated axospinous synapses with multiple, completely partitioned transmission zones: probable structural intermediates in synaptic plasticity. Hippocampus 3, 417–433.

Hammond, C., Crepel, V., Gozlan, H., Ben-Ari, Y., 1994. Anoxic LTP sheds light on the multiple facets of NMDA receptors. Trends Neurosci. 17, 497–503.

Harris, K.M., Jensen, F.E., Tsao, B., 1992. Three-dimensional structure of dendritic spines and synapses in rat hippocampus (CA1) at postnatal day 15 and adult ages: implications for the maturation of synaptic physiology and long-term potentiation. J. Neurosci. 12, 2685–2705.

Hartman, K.N., Pal, S.K., Burrone, J., Murthy, V.N., 2006. Activity-dependent regulation of inhibitory synaptic transmission in hippocampal neurons. Nat. Neurosci. 9, 642–649.

Hsu, K.S., Huang, C.C., 1997. Characterization of the anoxia-induced long-term synaptic potentiation in area CA1 of the rat hippocampus. Br. J. Pharmacol. 122, 671–681.

Jourdain, P., Nikonenko, I., Alberi, S., Muller, D., 2002. Remodeling of hippocampal synaptic networks by a brief anoxia-hypoglycemia. J. Neurosci. 22, 3108–3116.

Klausberger, T., Somogyi, P., 2008. Neuronal diversity and temporal dynamics: the unity of hippocampal circuit operations. Science 321, 53–57.

Knott, G.W., Quairiaux, C., Genoud, C., Welker, E., 2002. Formation of dendritic spines with GABAergic synapses induced by whisker stimulation in adult mice. Neuron 34, 265–273.

Kullmann, D.M., Lamsa, K.P., 2007. Long-term synaptic plasticity in hippocampal interneurons. Nat. Rev. Neurosci. 8, 687–699.

Marty, S., Wehrle, R., Sotelo, C., 2000. Neuronal activity and brain-derived neurotrophic factor regulate the density of inhibitory synapses in organotypic slice cultures of postnatal hippocampus. J. Neurosci. 20, 8087–8095.

Marty, S., Wehrle, R., Fritschy, J.M., Sotelo, C., 2004. Quantitative effects produced by modifications of neuronal activity on the size of GABAA receptor clusters in hippocampal slice cultures. Eur. J. Neurosci. 20, 427–440.

McBain, C.J., Kauer, J.A., 2009. Presynaptic plasticity: targeted control of inhibitory networks. Curr. Opin. Neurobiol. 19, 254–262.

Megias, M., Emri, Z., Freund, T.F., Gulyas, A.I., 2001. Total number and distribution of inhibitory and excitatory synapses on hippocampal CA1 pyramidal cells. Neuroscience 102, 527–540.

Miles, R., Toth, K., Gulyas, A.I., Hajos, N., Freund, T.F., 1996. Differences between somatic and dendritic inhibition in the hippocampus. Neuron 16, 815–823.

Nissen, W., Szabo, A., Somogyi, J., Somogyi, P., Lamsa, K.P., 2010. Cell type-specific long-term plasticity at glutamatergic synapses onto hippocampal interneurons expressing either parvalbumin or CB1 cannabinoid receptor. J. Neurosci. 30, 1337–1347.

Nusser, Z., Hajos, N., Somogyi, P., Mody, I., 1998. Increased number of synaptic GABA (A) receptors underlies potentiation at hippocampal inhibitory synapses. Nature 395, 172–177.

Pelletier, J.G., Lacaille, J.C., 2008. Long-term synaptic plasticity in hippocampal feedback inhibitory networks. Prog. Brain Res. 169, 241–250.

Peters, A., Palay, S., Webster, H.D., 1991. The Fine Structure of the Nervous System: Neurons and Their Supporting Cells, third ed. Oxford University Press, New York.

Saliba, R.S., Michels, G., Jacob, T.C., Pangalos, M.N., Moss, S.J., 2007. Activity-dependent ubiquitination of GABA(A) receptors regulates their accumulation at synaptic sites. J. Neurosci. 27, 13341–13351.

Somogyi, P., Klausberger, T., 2005. Defined types of cortical interneuron structure space and spike timing in the hippocampus. J. Physiol. 562, 9–26.

Stewart, M.G., Medvedev, N.I., Popov, V.I., Schoepfer, R., Davies, H.A., Murphy, K., Dallerac, G.M., Kraev, I.V., Rodriguez, J.J., 2005. Chemically induced long-term potentiation increases the number of perforated and complex postsynaptic densities but does not alter dendritic spine volume in CA1 of adult mouse hippocampal slices. Eur. J. Neurosci. 21, 3368–3378.

Stoppini, L., Buchs, P.A., Muller, D., 1991. A simple method for organotypic cultures of nervous tissue. J. Neurosci. Methods 37, 173–182.

Toni, N., Buchs, P.A., Nikonenko, I., Bron, C.R., Muller, D., 1999. LTP promotes formation of multiple spine synapses between a single axon terminal and a dendrite. Nature 402, 421–425.

Toni, N., Buchs, P.A., Nikonenko, I., Povilaitite, P., Parisi, L., Muller, D., 2001. Remodeling of synaptic membranes after induction of long-term potentiation. J. Neurosci. 21, 6245–6251.